

Search for CP violation and new physics in rare B decays at the B factories

G. Marchiori (giovanni.marchiori@lpnhe.in2p3.fr), on behalf of the BABAR and Belle Collaborations
 Laboratoire de Physique Nucléaire et de Hautes Energies (IN2P3/CNRS), 4 Place Jussieu, 75005 Paris, France

We summarize recent results by the BABAR and Belle Collaborations on the search for CP violation and new physics beyond the Standard Model in several rare B meson decays. The measurements exploit the final BABAR and Belle $\Upsilon(4S)$ dataset, which consist of approximately 470 and 772 million $B\bar{B}$ pairs, respectively.

I. INTRODUCTION

The B factory experiments, BABAR at SLAC and Belle at KEK, have been operated successfully in the first decade of the 21st century, collecting in total more than one billion pairs of charged (B^+B^-) and neutral ($B^0\bar{B}^0$) B mesons. Such large samples have been obtained from the decays of boosted $\Upsilon(4S)$ mesons produced in asymmetric e^+e^- collisions at $\sqrt{s} = m_{\Upsilon}$, $e^+e^- \rightarrow \Upsilon(4S) \rightarrow B\bar{B}$. After establishing experimentally CP violation in the B meson system and confirming the Cabibbo-Kobayashi-Maskawa (CKM) paradigm [1, 2] by measuring with good or excellent precision the sides and angles of the unitarity triangle in the “golden” modes, like $B \rightarrow c\bar{c}K^{(*)0}$ for the angle $\beta = \arg[-V_{cd}V_{cb}^*/V_{td}V_{tb}^*]$ ($\sin 2\beta = 0.679 \pm 0.020$ [3]), a significant fraction of the B factories’ physics program has been focused on rare B decays, which can provide additional constraints on the unitarity triangle parameters, or can probe the presence of new physics (NP) beyond the Standard Model (SM).

II. EXPERIMENTAL TECHNIQUES

Both BABAR and Belle are multi-purpose, (longitudinally) asymmetric detectors with nearly 4π coverage. In the e^+e^- collisions the $\Upsilon(4S)$ are produced with a Lorentz boost $\gamma\beta$ along the beam axis of 0.56 in BABAR and 0.42 in Belle, resulting in an average longitudinal separation between the two B decay vertices of ≈ 200 -250 microns, from which the proper time difference between the two decays can be inferred. The two detectors consist of an inner silicon detector to reconstruct B and D decay vertices and low- p_T charged particles, a gaseous drift chamber for charged particle tracking, various devices optimized for excellent charged particle identification (PID) at low energy (≈ 1 GeV) through various techniques (dE/dx , Cherenkov light, time of flight, ..), homogeneous scintillating electromagnetic calorimeters for e/γ reconstruction and identification, and muon and K_L detectors installed in the iron yoke used to contain the flux return of the solenoid that provides the magnetic field for tracking.

$B\bar{B}$ events produce typically a few number of charged (≈ 11) and neutral particles and often it is possible to fully reconstruct a B decay, *i.e.* to measure directly each of its decay products. This allows the calculation of two kinematic quantities characterizing the B meson, the energy-substituted invariant mass (m_{ES} or M_{bc}), $m_{ES} = \sqrt{(E_{\text{beam}}^*)^2 - (p_B^*)^2}$, and the energy difference, $\Delta E = E_B^* - E_{\text{beam}}^*$. For correctly reconstructed B decays, these two quantities peak around the B meson mass (m_B) and zero, respectively. Sometimes the B decay under study produces “invisible” particles that do not interact with the detector, for instance a neutrino or an hypothetical weakly interacting supersymmetric particle: in that case, one can still fully reconstruct the recoiling B (usually denoted as B_{tag}) and use it to infer the four-momentum of the signal B and of the invisible particles.

When a pair of neutral B mesons is produced, the flavors of the two mesons are entangled. If the first B meson decays at time t to a flavor specific final state, which can be identified through the presence of leptons, kaons or soft pions, the second B meson is inferred to have at the same time t the opposite flavor. These correlations are exploited in time-dependent CP violation measurements.

The e^+e^- collisions can also produce light quark-antiquark pairs, $q\bar{q}$ ($q = u, d, s, c$). The $B\bar{B}$ production cross section is around one fifth of the total hadronic cross section. The hadronic $q\bar{q}$ backgrounds are typically distinguished from $B\bar{B}$ events by means of event-shape variables, that discriminate between the “jet-like” topology of $q\bar{q}$ events

TABLE I: Results of the $B \rightarrow \eta h$ measurements by the Belle Collaboration [13].

Decay	BF (10^{-6})	BF significance (σ)	A_{CP}	A_{CP} significance (σ)
$B^+ \rightarrow \eta K^+$	$2.12 \pm 0.23 \pm 0.11$	13.2	$-0.38 \pm 0.11 \pm 0.01$	3.8
$B^+ \rightarrow \eta \pi^+$	$4.07 \pm 0.26 \pm 0.21$	22.4	$-0.19 \pm 0.06 \pm 0.01$	3.0
$B^0 \rightarrow \eta K^0$	$1.27^{+0.33}_{-0.29} \pm 0.08$	5.4	–	–

and the more “spherical” $B\bar{B}$ events, and also exploit the different angular distributions expected from angular momentum conservation and spin arguments. Because of the large correlations between the shape variables, those are usually combined in a single discriminating quantity using multivariate techniques (Fisher discriminants, neural networks), trained on clean samples of $q\bar{q}$ events collected at $\sqrt{s} \approx 40 - 50$ MeV below the $\Upsilon(4S)$ peak and with simulated signal samples.

III. SEARCH FOR CP VIOLATION IN CHARMLESS B DECAYS

Charmless hadronic B decays provide sensitive probes for CP violation in the Standard Model and beyond, since:

- large CP -violating effects are predicted by the SM in some of these channels, and can therefore be measured with good precision;
- the amount of CP violation in some charmless B decays is related, in the SM, to the amount of CP violation – measured with excellent precision – in $B^0 \rightarrow (c\bar{c})K^0$ decays;
- some of these decays proceeds mainly (or purely) through loop-mediated diagrams and SM predictions could therefore be significantly affected by possible new physics contributions appearing in the loops of these diagrams.

A. Search for CP violation in two-body $B \rightarrow \eta h$ ($h = \pi^+, K^+, K^0$) decays

Calculations of the SM contributions to the $B \rightarrow \eta K$ and $B \rightarrow \eta \pi$ decays, combined with the measured values of the $B^\pm \rightarrow \eta^{(\prime)} K^\pm$ and $B^0 \rightarrow \eta' K^0$ branching fractions, lead to the following expectations [4–12]:

1. the branching fraction of $B^0 \rightarrow \eta K^0$ is expected to be lower than that of $B^\pm \rightarrow \eta K^\pm$, because the tree diagram in the $B^0 \rightarrow \eta K^0$ decay is color suppressed.
2. in $B^\pm \rightarrow \eta K^\pm$, a large direct CP asymmetry (A_{CP}) is expected, as a consequence of the interference between the destructive combination of penguin amplitudes and the tree amplitude.
3. in $B^\pm \rightarrow \eta \pi^\pm$, a large A_{CP} is also anticipated, due to the interference between the $b \rightarrow d$ penguin and $b \rightarrow u$ tree diagrams.

Belle has published in [13] an updated measurement of $B \rightarrow \eta h$ ($h = \pi^+, K^+, K^0$) decays[36] using the final data sample of 772×10^6 $B\bar{B}$ pairs. The η meson is reconstructed in both the $\pi^+\pi^-\pi^0$ and $\gamma\gamma$ final states, while the K^0 meson is selected as a K_S^0 decaying to two oppositely-charged pions. The full B decay tree is reconstructed, with an efficiency – including secondary branching fractions – of around 1.5% (4%) for the ηK^0 and 5% (14%) for the ηh^+ final states, in the $\eta \rightarrow \pi^+\pi^-\pi^0$ ($\eta \rightarrow \gamma\gamma$) channel. The signal yield is obtained through a maximum likelihood (ML) fit to M_{bc} , ΔE and an event-shape variable R' . The samples containing the ηK^+ and $\eta \pi^+$ candidates are fitted simultaneously, in order to constrain the background from the $\eta K \leftrightarrow \eta \pi$ cross-feed. The projections of the fit on the M_{bc} variable for $B^+ \rightarrow \eta K^+$ and $B^- \rightarrow \eta K^-$ candidates, selected after further enhancing S/B with the requirements $-0.1 < \Delta E < 0.08$ GeV and $R' > 1.95$, are shown in Figure 1.

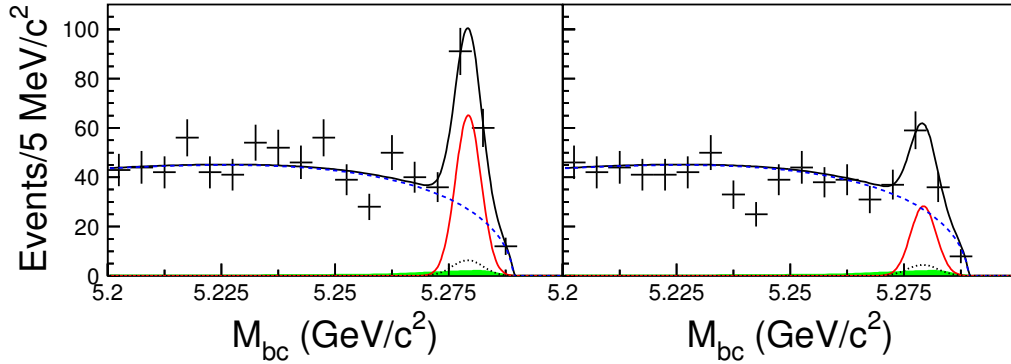


FIG. 1: M_{bc} projections for $B^+ \rightarrow \eta K^+$ (left) and $B^- \rightarrow \eta K^-$ (right) candidate events selected by Belle [13]. Points with error bars represent the data, the total fit functions are shown by black solid curves, signals are shown by red solid curves, dashed curves are the continuum contributions, dotted curves are the cross-feed backgrounds from misidentification and filled histograms are the contributions from charmless B backgrounds. The projections are for events that have $-0.10 < \Delta E < 0.08$ GeV and $R' > 1.95$.

The main results are summarized in Table I. Both $B^+ \rightarrow \eta K^+$ and $B^+ \rightarrow \eta \pi^+$ signals are observed with large statistical significances, exceeding 10σ and 20σ respectively, and both B decays exhibit large negative CP asymmetries, around -40% and -20% respectively, at least 3σ different from zero. The $B \rightarrow \eta K^0$ decay is observed for the first time, with a significance of more than 5σ , and its branching fraction is smaller than that of $B^+ \rightarrow \eta K^+$. All results are in agreement with SM expectations.

B. Search for CP violation in three-body $B \rightarrow KKK$ decays

Measurements of time-dependent CP violation in $b \rightarrow q\bar{q}s$ ($q = u, d, s$) decays offer a method for determining β alternative to the one based on $B \rightarrow c\bar{c}K^{(*)0}$. Such decays are dominated by $b \rightarrow s$ loop diagrams, and therefore are sensitive to possible new physics contributions appearing in the loops of these diagrams. As a result, the effective β (β_{eff}) measured in such decays could differ from β measured in $B^0 \rightarrow c\bar{c}K^0$. Two final states, the CP -even $K_S^0 K_S^0 K_S^0$ and the CP -odd ϕK_S^0 , are particularly suited for a NP search, as β_{eff} for these decays is expected to be very close, within a few %, to β measured in B decays to charmonium [14–16], with very little theoretical uncertainties. The related decay mode $B^\pm \rightarrow \phi K^\pm$ is also a powerful probe to NP, since it is dominated in the SM by a single $b \rightarrow s$ penguin amplitude, and its direct CP asymmetry is predicted to be small, $A_{CP} \approx (0.0 - 4.7)\%$.

BABAR has published in [17] a detailed study of $B \rightarrow K_S^0 K_S^0 K_S^0$ decays, including a time-integrated, CP -averaged Dalitz plot analysis – to extract the amplitude and phases of the various resonant and non-resonant contributions to the decay – and a measurement of $\sin 2\beta_{\text{eff}}$ from the time-dependent CP asymmetry. In the Dalitz plot analysis, events are selected in which three K_S^0 decay to charged pion pairs, have a common vertex and form a B meson candidate with $m_{\text{ES}} \approx m_B$ and $\Delta E \approx 0$. Continuum $q\bar{q}$ background is suppressed by means of a neural network NN of four event-shape variables. The $B^0 \rightarrow K_S^0 K_S^0 K_S^0$ decay amplitude is modeled as the sum of a non-resonant term and several intermediate two-body amplitudes; the magnitudes and phases of each term are determined, together with the signal and background yields, through a maximum likelihood fit to m_{ES} , ΔE , NN , and to the two Dalitz plot variables, s_{min} and s_{max} , which are the minimum and the maximum, respectively, among the three Mandelstam variables s_{ij} , where the indices $i, j = 1, 2, 3$ ($i \neq j$) denote the three K_S^0 . Evidence is found for contributions to the final state by $f_0(980)K_S^0$, $f_0(1710)K_S^0$, $f_2(2010)K_S^0$, $\chi_{c0}K_S^0$ and non-resonant $K_S^0 K_S^0 K_S^0$, while the fit likelihood does not improve significantly when including in the model additional resonances, like the broad $f_X(1500)$ used to explain some older data [18]. The global maximum of the likelihood favors large non-resonant and small resonant contributions, with significant destructive interference among them. The signal yield obtained from the fit is 200 ± 15 , while the efficiency, obtained from a simulation of signal events where the magnitudes and phases of the intermediate

resonances are fixed to the central values returned by the fit, is $\varepsilon = 6.6\%$, yielding an inclusive branching fraction $BF(B^0 \rightarrow K_S^0 K_S^0 K_S^0) = (6.19 \pm 0.48 \pm 0.15 \pm 0.12) \times 10^{-6}$.

In the CP violation analysis, events are selected in which one neutral B_{tag} decays to a (partially reconstructed) flavor-specific final state, thus identifying the flavor of the other B (B_{sig}) as B^0 or \bar{B}^0 at the same time, while B_{sig} decays to either three $K_S^0 \rightarrow \pi^+ \pi^-$ ($\varepsilon = 6.6\%$) or two $K_S^0 \rightarrow \pi^+ \pi^-$ and one $K_S^0 \rightarrow \pi^0 \pi^0$ ($\varepsilon = 3.1\%$). The CP asymmetry between the B^0 and \bar{B}^0 decays to three K_S^0 has a dependence on the proper time difference Δt between the two B decays of the form $[\mathcal{S} \sin(\Delta m_d \Delta t) - \mathcal{C} \cos(\Delta m_d \Delta t)]$, where Δm_d is the mass difference between the two neutral B physical eigenstates. In the SM $\mathcal{S} = -\sin 2\beta$, while $\mathcal{C} \approx 0$, since the decay amplitude is dominated by a single weak phase term and direct CP violation is thus negligible. \mathcal{S} and \mathcal{C} are extracted from a maximum likelihood fit to Δt , m_{ES} , ΔE and NN for the selected candidates (see Figure 2). The signal yield is 263 ± 21 , and the measured values of \mathcal{S} and \mathcal{C} are:

$$\mathcal{S} = -0.94_{-0.21}^{+0.24}(\text{stat}) \pm 0.06(\text{syst}), \quad (1)$$

$$\mathcal{C} = -0.17 \pm 0.18(\text{stat}) \pm 0.24(\text{syst}), \quad (2)$$

where the systematic errors are dominated by the Δt resolution and the fit bias. They are compatible within two standard deviations with those measured in tree-dominated modes such as $B^0 \rightarrow J/\psi K_S^0$, as expected in the SM. CP conservation ($\mathcal{S} = \mathcal{C} = 0$) is excluded at 3.8σ , including systematic uncertainties, thus providing for the first time evidence of CP violation in $B^0 \rightarrow K^0 K^0 K^0$ decays.

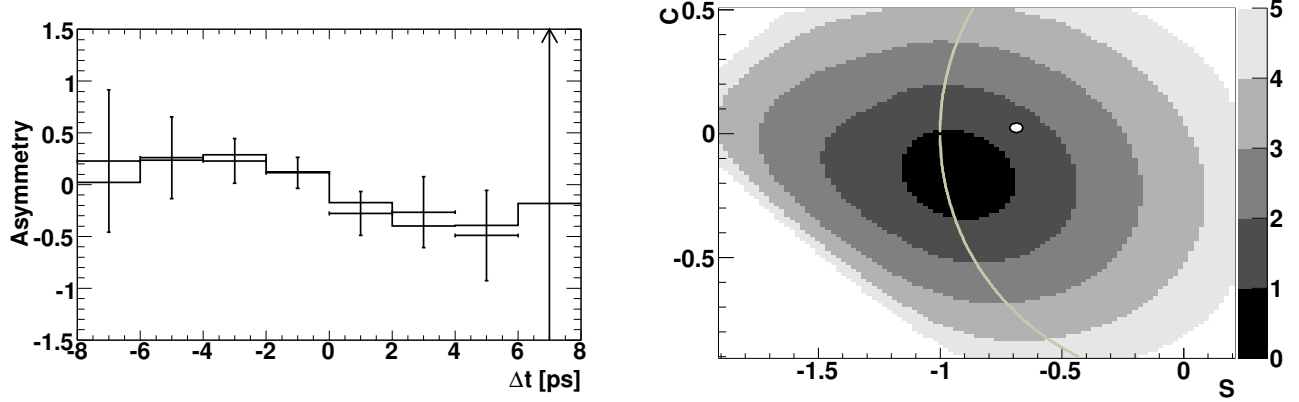


FIG. 2: Left: Background-subtracted data distribution (points with error bars) and fit (histogram) of the time-dependent CP asymmetry for $B \rightarrow K_S^0 K_S^0 K_S^0$ candidates reconstructed by BABAR [17]. Right: two-dimensional scan of $-2\Delta \ln \mathcal{L}$, including systematic uncertainties, as a function of \mathcal{S} and \mathcal{C} . The result of the BABAR analysis of $B^0 \rightarrow c\bar{c}K^{(*)}$ decays is indicated as a white ellipse and the physical boundary ($\mathcal{S}^2 + \mathcal{C}^2 \leq 1$) is marked as a gray line.

BABAR has also published in [19] a detailed study of the other B decays to three kaons. The decay $B^0 \rightarrow K^+ K^- K_S^0$ is used, by performing a time-dependent analysis, to measure β_{eff} in B^0 decays to the CP -odd final state ϕK_S^0 and also to the (mostly CP -even) other resonant and non-resonant $K^+ K^- K_S^0$ final states. The decay $B^0 \rightarrow K^+ K^- K^+$ is used to determine the direct CP asymmetry in $B^+ \rightarrow \phi K^+$. In order to disentangle the $B \rightarrow \phi K$ contribution from other resonant or non-resonant contributions, a Dalitz plot analysis is performed for each of the final states considered. In addition, to better understand the Dalitz plot structure of these decays and the possible intermediate KK resonances, also $B^+ \rightarrow K_S^0 K_S^0 K^+$ decays are studied, since they have a simplified spin structure due to the fact that the two K_S^0 mesons in the final state are forbidden (by Bose–Einstein statistics) to be in an odd angular momentum configuration. Events with three charged or neutral kaons kinematically consistent with a B decay (common production vertex, $m_{\text{ES}} \approx m_B$, $\Delta E \approx 0$) are selected. Continuum background events are suppressed by means of a neural network NN of typically five event-shape variables. The signal B decay amplitude is modeled as the sum of a non-resonant and of several resonant contributions, whose magnitudes and phases are determined

through a maximum likelihood fit to the Dalitz plot variables, together with m_{ES} , ΔE and NN . Only resonances that significantly improve the quality of the fit are kept in the nominal signal decay amplitude: in all the three channels no evidence is found for the broad $f_X(1500)$. The selection efficiency is around 30% for each of the three decay modes. The number of selected signal decays, the measured inclusive charmless branching fractions (excluding the $\chi_{c0}K$ contributions) and the CP -violating parameters are summarized in Table II. Some of the fit results are also illustrated in Figures 3 and 4. The CP asymmetry in $B^+ \rightarrow \phi K^+$ differs from 0 by 2.8σ , and is in slight tension with SM predictions ($0 - 4.7\%$). The amount of CP violation in $B^0 \rightarrow \phi K_S^0$ and in other $B^0 \rightarrow K^+K^-K_S^0$ decays is in excellent agreement with SM expectations: β_{eff} is very close to β measured in B decays to charmonium, and \mathcal{C} is consistent with zero.

TABLE II: Results of the $B \rightarrow KKK$ measurements by the BABAR Collaboration [19]. For neutral B decays, the CP asymmetry A_{CP} is defined as $A_{CP} = -\mathcal{C}$.

Decay	N_{sig}	BF (10^{-6})	A_{CP}	β_{eff}
$B^+ \rightarrow K^+K^-K^+$	5269 ± 84	$33.4 \pm 0.5 \pm 0.9$	$(-1.7^{+1.9}_{-1.4} \pm 1.4)\%$ (inclusive) $(12.8 \pm 4.4 \pm 1.3)\%$ (ϕK^+)	—
$B^0 \rightarrow K^+K^-K_S^0$	1579 ± 46	$25.4 \pm 0.9 \pm 0.8$	$(-5 \pm 18 \pm 5)\%$ (ϕK_S^0) $(-28 \pm 24 \pm 9)^\circ$ ($f_0(980)K_S^0$) $(-2 \pm 9 \pm 3)^\circ$ (Other)	$(21 \pm 6 \pm 2)^\circ$ (ϕK_S^0) $(18 \pm 6 \pm 4)^\circ$ ($f_0(980)K_S^0$) $(20.3 \pm 4.3 \pm 1.2)^\circ$ (Other)
$B^+ \rightarrow K_S^0K_S^0K^+$	632 ± 28	$10.1 \pm 0.5 \pm 0.3$	$(4 \pm 5 \pm 2)\%$	—

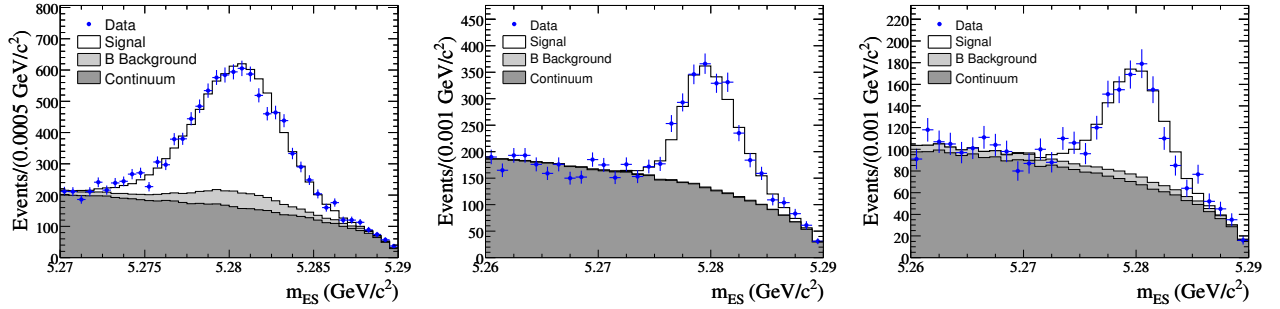


FIG. 3: Distributions of m_{ES} for $B^+ \rightarrow K^+K^-K^+$ (left), $B^0 \rightarrow K^+K^-K_S^0$, and $B^+ \rightarrow K_S^0K_S^0K^+$ (right) selected by BABAR [19] (points with error bars). The fit results are overlaid.

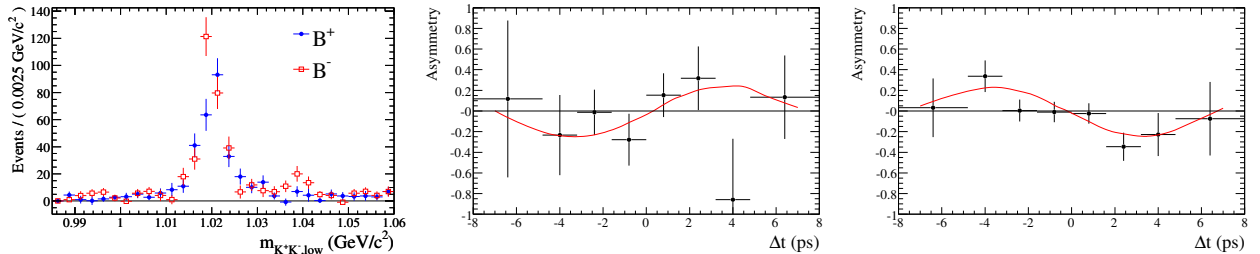


FIG. 4: Left: Background-subtracted distributions of $B^\pm \rightarrow K^+K^-K^\pm$ candidates in data, plotted separately for B^+ and B^- events, in the “ $\phi(1020)$ region” where $m_{K^+K^-} \approx m_\phi$ (considering the kaon pair with lowest invariant mass). Center and right: time-dependent CP asymmetry, as a function of Δt , for $B^0 \rightarrow K^+K^-K_S^0$ candidates in the $\phi(1020)$ region (center) and in the $\phi(1020)$ -excluded region (right). The points represent signal-weighted data, and the line is the fit model.

C. Search for CP violation in three-body $B \rightarrow K\pi^0\pi^0$ decays

Recent measurements of rates and asymmetries in $B \rightarrow K\pi$ decays may hint to possible new physics contributions, but hadronic uncertainties prevent a clear conclusion in this direction. Additional information can be obtained through a data-driven approach involving measurements of all the observables in the $B \rightarrow K\pi$ system, or looking at the related pseudoscalar-vector decays $B \rightarrow K^*\pi$ and $B \rightarrow K\rho$. In such decays, the ratios of tree-to-penguin amplitudes are predicted to be 2 to 3 times larger than those in $B \rightarrow K\pi$, possibly leading to larger CP asymmetries [20–22].

BABAR has published in [23] a measurement of the branching fraction and CP asymmetry of the decay $B^\pm \rightarrow K^*(892)^\pm\pi^0$, based on the final $\Upsilon(4S)$ sample. The $K^*(892)^+$ is reconstructed in the $K^+\pi^0$ decay channel, and discrimination between $B^+ \rightarrow K^*(892)^+\pi^0$ decays and other (resonant or non-resonant) $B^+ \rightarrow K^+\pi^0\pi^0$ decays is achieved through inspection of the two-body invariant mass distributions of the particles in the final state, since the Dalitz plot of this decay is characterized by rather narrow resonances ($K^*(892)^+$, $f_0(980)$, χ_{c0}). A total $B^+ \rightarrow$

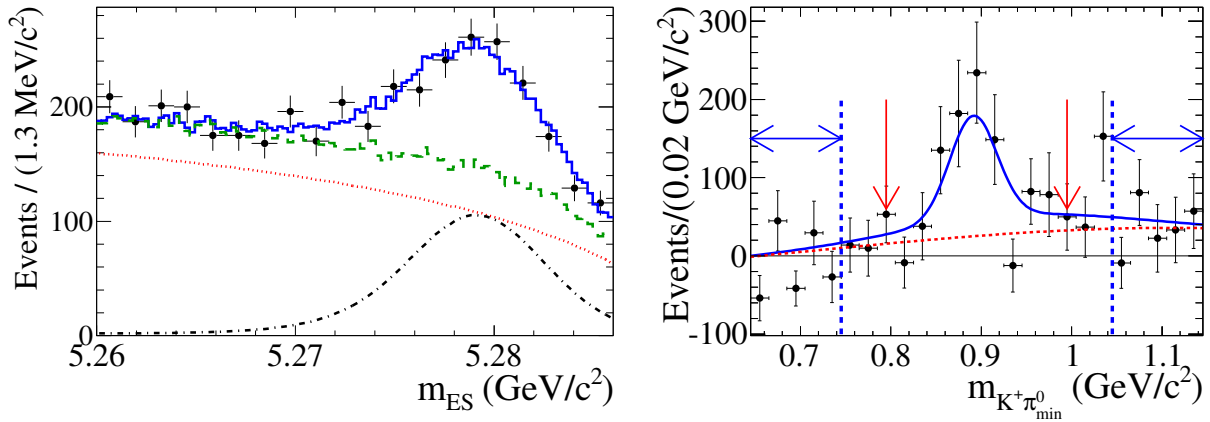


FIG. 5: Left: m_{ES} distribution of $B^\pm \rightarrow K^\pm\pi^0\pi^0$ candidates selected in data by *BABAR* [23], after applying a requirement on the neural-network variable that retains 60% of the signal while suppressing a large fraction of the $q\bar{q}$ background. The solid (blue) lines represents the m_{ES} projection of the total fit, the dashed (green) lines the total background contribution, and the dotted (red) lines the $q\bar{q}$ component. The dash-dotted lines represent the signal contribution. Right: efficiency-corrected, background-subtracted distribution of the invariant mass $m_{K^+\pi^0_{\min}}$ for $B^\pm \rightarrow K^\pm\pi^0\pi^0$ candidates where $m_{K^+\pi^0_{\min}}$ is close to the $K^*(892)^+$ mass. $m_{K^+\pi^0_{\min}}$ is the mass of the $K^+\pi^0$ combination with lower invariant mass. The vertical red arrows define the limits of the signal region while the blue horizontal arrows define the sideband background control regions. The curves show the results of the fit used to cross-check the procedure, for the total (blue solid line) and background-only (red dashed line) components.

$K^+\pi^0\pi^0$ yield of 1220 ± 85 events (significance $> 10\sigma$) is obtained from a ML fit to m_{ES} and to a neural network NN of event-shape variables (see Figure 5, left). The contribution from $B^+ \rightarrow K^*(892)^+\pi^0$ is obtained by subtracting non- $B^+ \rightarrow K^+\pi^0\pi^0$ events using the *sPlot* technique and then studying the distribution of $m_{K^+\pi^0_{\min}}$, the invariant mass of the $K^+\pi^0$ combination with lower invariant mass. The sidebands of $m_{K^+\pi^0_{\min}}$ are used to estimate the non- $K^*(892)^+\pi^0$ background in the signal region near the $K^*(892)^+$ mass, which is then subtracted from the number of candidates observed in the signal $m_{K^+\pi^0_{\min}}$ region (see Figure 5, right). The final results are summarized in Table III. For $B^\pm \rightarrow K^*(892)^\pm\pi^0$, a branching fraction of $(8.2 \pm 1.5 \pm 1.1) \times 10^{-6}$ is measured, with a CP asymmetry close to zero (-6%) but also consistent, within errors, with large CP violation ($A_{CP} \approx 20 - 30\%$) as expected in the SM.

TABLE III: Summary of measurements of branching fractions (averaged over charge conjugate states) and CP asymmetries measured by BABAR in $B^+ \rightarrow K^+ \pi^0 \pi^0$ decays [23]. Both product branching fractions and those corrected for secondary decays are shown. For each result, the first uncertainty is statistical, the second is systematic and the third, where quoted, is the error on $\chi_{c0} \rightarrow \pi^0 \pi^0$. The notation Rh refers, where applicable, to the intermediate state of a resonance and a bachelor hadron.

Decay	$BF(B^+ \rightarrow Rh \rightarrow K^+ \pi^0 \pi^0)(10^{-6})$	$BF(B^+ \rightarrow Rh)(10^{-6})$	A_{CP}
$B^+ \rightarrow K^+ \pi^0 \pi^0$	$16.2 \pm 1.2 \pm 1.5$	–	$-0.06 \pm 0.06 \pm 0.04$
$B^+ \rightarrow K^*(892)\pi^0$	$2.7 \pm 0.5 \pm 0.4$	$8.2 \pm 1.5 \pm 1.1$	$-0.06 \pm 0.24 \pm 0.04$
$B^+ \rightarrow f_0(980)K^+$	$2.8 \pm 0.6 \pm 0.5$	–	$0.18 \pm 0.18 \pm 0.04$
$B^+ \rightarrow \chi_{c0}K^+$	$0.51 \pm 0.22 \pm 0.09$	$180 \pm 80 \pm 30 \pm 10$	$-0.96 \pm 0.37 \pm 0.04$

IV. SEARCH FOR NEW PHYSICS IN VERY RARE B DECAYS

Some B meson decays are expected in the Standard Model to have branching fractions below the experimental sensitivity of the B -factories. The observation of such very rare decays would therefore provide evidence for new physics beyond the SM. This is the case for instance of lepton-flavor violating B decays and leptonic $B \rightarrow \nu\bar{\nu}$ decays.

A. Search for lepton flavor violation in $B \rightarrow h\tau\ell$

Lepton flavor violating decays of B mesons can occur in the SM through loop processes that involve neutrino mixing. These are highly suppressed by powers of m_ν^2/m_W^2 , and have predicted branching fractions many orders of magnitude below the current experimental sensitivity. However, in many extensions of the SM, B decays involving lepton flavor violation are greatly enhanced. In some cases, decays involving the second and third generations of quarks and leptons are particularly sensitive to physics beyond the SM [24–27].

BABAR has presented at the FPCP 2012 conference, and later published in [28], a search for the eight lepton flavor violating decays $B^\pm \rightarrow h^\pm \tau \ell$, $h = \pi, K$, $\ell = e, \mu$, using the final $\Upsilon(4S)$ dataset. Events in which one B meson (B_{tag}) is fully reconstructed in one of several hadronic final states, $B_{\text{tag}} \rightarrow D^{(*)0} n_1 \pi^\pm n_2 K^\pm n_3 K_S^0 n_4 \pi^0$, are selected. The number of tracks from the signal B (B_{sig}) decay and their particle identification information are required to be consistent with that of a $B^\pm \rightarrow h^\pm \tau \ell$ decay followed by a one-prong τ decay (producing either a charged electron, muon, or pion), in order to improve the signal-to-background ratio. Continuum background is suppressed using a likelihood ratio based on event shape information, unassociated calorimeter clusters, and the quality of muon identification for channels that have a muon in the final state. Background from semileptonic B or D decays is suppressed by rejecting events where two oppositely-charged B_{sig} daughters are found to be kinematically compatible with originating from a charm decay, by computing their invariant mass in the hypothesis of a $K\pi$ pair. Using the momenta of the reconstructed B , h , and ℓ candidates, the four momentum of the τ lepton in the center-of-mass frame is fully determined, thus circumventing the problem of measuring the undetected neutrino(s) from the τ decay:

$$\vec{p}_\tau^* = -\vec{p}_{\text{tag}}^* - \vec{p}_h^* - \vec{p}_\ell^* \quad (3)$$

$$E_\tau^* = E_{\text{beam}}^* - E_h^* - E_\ell^* \quad (4)$$

The resulting τ candidate mass, $m_\tau = \sqrt{E_\tau^{*2} - |\vec{p}_\tau^*|^2}$, is then used to discriminate against combinatorial background (see Figure 6). A broad m_τ sideband ($[0, 3.5]$ GeV/ c^2) is used to estimate the background in the signal region of m_τ close to the PDG τ mass, using a simulation of background events to relate the number of background candidates in the sideband region to the number of background candidates in the signal region. To reduce systematic uncertainties, the signal branching fraction is determined by using the ratio of the number of $B \rightarrow h\tau\ell$ signal candidates to the

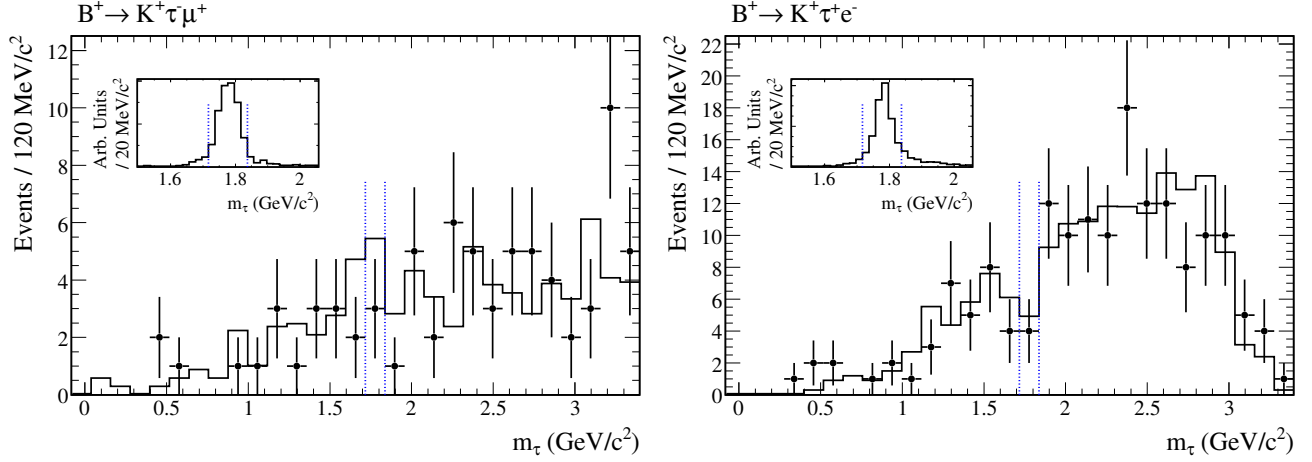


FIG. 6: Observed distributions of the τ invariant mass for the $B^+ \rightarrow K^+ \tau^- \mu^+$ candidates (left) and the $B^+ \rightarrow K^+ \tau^- e^-$ candidates (right) selected by BABAR [28]. The distributions show the sum of the three τ channels (e, μ, π). The points with error bars are the data. The solid line is the background MC which has been normalized to the area of the data distribution. The dashed vertical lines indicate the m_τ signal window range. The inset shows the m_τ distribution for signal MC.

yield of control samples of $B^- \rightarrow D^{(*)0} \ell^- \bar{\nu}$, $D^0 \rightarrow K^- \pi^+$ decays in events with a fully reconstructed hadronic B_{tag} :

$$BF_{h\tau\ell} = BF_{D\ell\nu} \frac{N_{h\tau\ell} \varepsilon_{D\ell\nu}^{\text{sig}} \varepsilon_{D\ell\nu}^{\text{tag}}}{N_{D\ell\nu} \varepsilon_{h\tau\ell}^{\text{sig}} \varepsilon_{h\tau\ell}^{\text{tag}}}. \quad (5)$$

Here $\varepsilon_{h\tau\ell}^{\text{tag}}$ and $\varepsilon_{D\ell\nu}^{\text{tag}}$ are the (similar) B_{tag} reconstruction efficiencies for events containing the different B_{sig} decays, while $\varepsilon_{h\tau\ell}^{\text{sig}}$ and $\varepsilon_{D\ell\nu}^{\text{sig}}$ are the signal selection efficiencies. A charged B_{tag} candidate is properly reconstructed in approximately 0.25% of all $B\bar{B}$ events. The $B \rightarrow h\tau\ell$ selection efficiency varies between 2% and 10% depending on the final state; the $D^{(*)0} \ell\nu$ signal efficiencies are close to 50%. The $D^0 \ell\nu$ and $D^{*0} \ell\nu$ yields are determined through a fit to the energy difference of the selected candidates,

$$\Delta E_{D\ell\nu} = E_K^* + E_\pi^* + E_\ell^* + E_\nu^* - E_{\text{beam}}^*, \quad (6)$$

where $E_\nu^* = p_\nu^* = |-\vec{p}_{\text{tag}}^* - \vec{p}_K^* - \vec{p}_\pi^* - \vec{p}_\ell^*|$. The energy difference is peaked at 0 for $B \rightarrow D^0 \ell\nu$ and is peaked at lower values (≈ -200 MeV) for $B \rightarrow D^{*0} \ell\nu$ (because of the undetected γ or π^0 from the D^{*0} decay), while $B \rightarrow D^{*0} \ell\nu$ and other backgrounds do not peak in $\Delta E_{D\ell\nu}$ (see Figure 7).

No evidence for the $B \rightarrow h\tau\ell$ decays is found, and 90% confidence level upper limits are set – with a frequentist technique – on each branching fraction at the level of a few times 10^{-5} , as summarized in Table IV. The results are used to improve model-independent limits on the energy scale of new physics in flavor-changing sermonic effective operators [26] to $\Lambda_{bd} > 11$ TeV and $\Lambda_{bs} > 15$ TeV.

B. Search for new physics in B^0 decays to invisible final states and to $\nu\bar{\nu}\gamma$

The decay $B^0 \rightarrow \nu\bar{\nu}$, which would give an invisible experimental signature, is strongly helicity-suppressed in the SM by a factor of order $(m_\nu/m_B)^2$ and its branching fraction is thus well below the B factory experimental observability [29]. The SM expectation for the $B^0 \rightarrow \nu\bar{\nu}\gamma$ branching fraction is predicted to be of order 10^{-9} , with very little uncertainty from hadronic interactions [30]. An experimental observation of an invisible ($+\gamma$) decay of a B^0 at the B factories would thus be a clear sign of physics beyond the SM. Supersymmetric models or models with large extra dimensions allow significant, although small, rates for invisible B^0 decays, with branching fractions up to the $10^{-7} - 10^{-6}$ range [31–33].

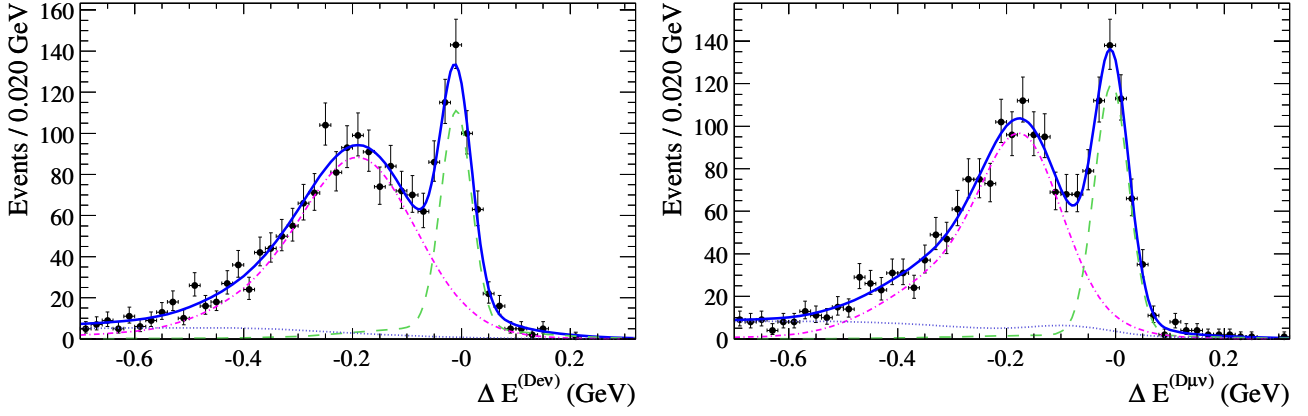


FIG. 7: Distributions of the three-component $\Delta E_{D\ell\nu}$ unbinned maximum likelihood fits of the data for the $B \rightarrow D^{(*)0}e\nu$ (left) and $B \rightarrow D^{(*)0}\mu\nu$ (right) control samples selected in the $B \rightarrow h\tau\ell$ BABAR analysis [28]. In each plot, the points represent the data, the solid blue curve is the fit result, the long-dashed green curve is the D^0 component, the dash-dotted purple curve is the D^{*0} component, and the dotted blue curve is the D^{*0} component, which also includes any residual combinatorial background.

TABLE IV: Branching fraction central values and 90% C.L. upper limits (UL) for $BF(B^+ \rightarrow h^+\tau\ell)$. The uncertainties include statistical and systematic sources.

Mode	$BF(B \rightarrow h\tau\ell) (\times 10^{-5})$	
	central value	90% C.L. UL
$B^+ \rightarrow K^+\tau^-\mu^+$	$0.8^{+1.9}_{-1.4}$	< 4.5
$B^+ \rightarrow K^+\tau^+\mu^-$	$-0.4^{+1.4}_{-0.9}$	< 2.8
$B^+ \rightarrow K^+\tau^-e^+$	$0.2^{+2.1}_{-1.0}$	< 4.3
$B^+ \rightarrow K^+\tau^+e^-$	$-1.3^{+1.5}_{-1.8}$	< 1.5
$B^+ \rightarrow \pi^+\tau^-\mu^+$	$0.4^{+3.1}_{-2.2}$	< 6.2
$B^+ \rightarrow \pi^+\tau^+\mu^-$	$0.0^{+2.6}_{-2.0}$	< 4.5
$B^+ \rightarrow \pi^+\tau^-e^+$	$2.8^{+2.4}_{-1.9}$	< 7.4
$B^+ \rightarrow \pi^+\tau^+e^-$	$-3.1^{+2.4}_{-2.1}$	< 2.0

Both Belle and BABAR have presented at the FPCP 2012 conference preliminary results on invisible B^0 decays; BABAR has also searched for $B^0 \rightarrow \nu\bar{\nu}\gamma$ decays. The results have been later publicly documented in [34] and [35]. The analysis technique is similar for the two experiments: only events where a neutral B_{tag} meson is found are considered, and the rest of the event (the “signal side”) is checked for consistency with an invisible decay or a decay to a single photon of the other neutral B . Events with extra tracks or neutral pions or K_L^0 candidates are vetoed. The total energy E_{extra} (or E_{ECL}) in the electromagnetic calorimeter, computed in the CM frame and not associated with neutral particles or charged tracks used in the B_{tag} reconstruction, is used to discriminate between signal and background. For $B^0 \rightarrow \text{invisible} + \gamma$, the energy of the highest-energy photon remaining in the event is also removed from the E_{extra} computation. In signal events E_{extra} is strongly peaked at zero, while for the background its distribution increases uniformly with E_{extra} . The main difference between the Belle and BABAR analyses is that Belle performs a full reconstruction of the B_{tag} candidate in hadronic final states, while BABAR opts for a partial reconstruction in the $D^{(*)-}\ell^+\nu$ decays. The latter has the advantage of a higher reconstruction efficiency with respect to the former (by a factor ≈ 10 : the $B \rightarrow \text{invisible}$ efficiency is 0.18% for BABAR and 0.022% for Belle), but has the disadvantage of the presence of the invisible neutrino, which prevents the exploitation of kinematic variables such as the reconstructed B^0 mass. S/B is therefore worse in the case of the partial B_{tag} reconstruction, though the background contamination is mitigated by the presence of a high momentum lepton.

The signal yield is extracted from a maximum likelihood fit to the two-dimensional distributions of E_{ECL} and of an event-shape variable, $\cos\theta_B$ (Belle), or to the one-dimensional E_{extra} distribution (BABAR), as illustrated in Figures 8 and 9. No evidence for $B \rightarrow \text{invisible}(+\gamma)$ decays is found, and 90% confidence level upper limits are set – with a Bayesian technique – on each branching fraction, at the level of a few times 10^{-5} , as summarized in Table V. The Belle limit is a factor ≈ 5 worse than BABAR because of the lower efficiency of the hadronic tag full reconstruction.

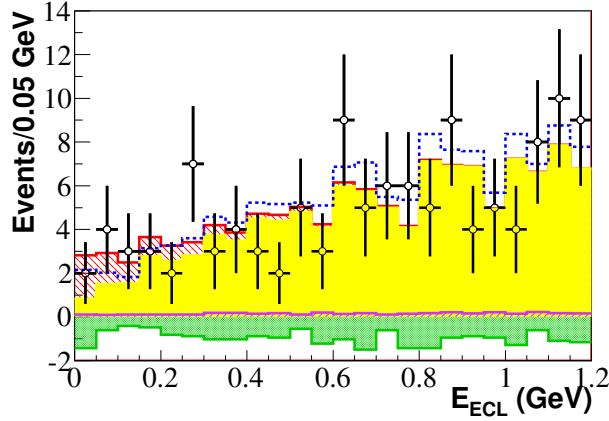


FIG. 8: E_{ECL} distribution of $B \rightarrow \text{invisible}$ candidates (points) selected by Belle, with fit results superimposed. The red cross-hatched region is the signal component, on the top of the total background shown in the yellow filled histogram. The blue dashed curve is the generic B contribution, which is larger than the total because of the negative fit result for the non-B background shown in the green dotted histogram. The purple hatched area corresponds to the rare B contribution.

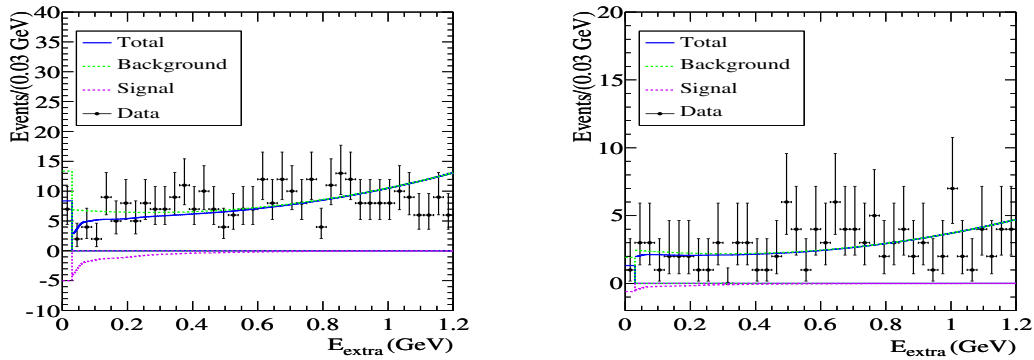


FIG. 9: E_{extra} distributions of $B \rightarrow \text{invisible}$ (left) and $B \rightarrow \text{invisible} + \gamma$ (right) candidates selected by BABAR (points), with fit results superimposed: signal (purple dotted line), background (green, dotted line) and sum of signal and background (blue solid line).

TABLE V: 90% C.L. upper limits on the branching fractions of $B \rightarrow \text{invisible}(+\gamma)$ decays measured by the Belle and BABAR collaborations [34, 35].

Decay	BF (Belle)	BF (BABAR)
$B^0 \rightarrow \text{invisible}$	$< 13 \times 10^{-5}$	$< 2.4 \times 10^{-5}$
$B^0 \rightarrow \text{invisible} + \gamma$	–	$< 1.7 \times 10^{-5}$

V. CONCLUSION

Several results on rare B decays obtained at the B factories have been discussed. The main results are:

- CP violation has been observed with $> 3\sigma$ significance in $B^\pm \rightarrow \eta K^\pm$ and $B^\pm \rightarrow \eta \pi^\pm$. Large CP asymmetries are observed. $B^0 \rightarrow \eta K^0$ is observed for the first time, with a branching fraction smaller than that of $B^+ \rightarrow \eta K^+$.
- CP -violation parameters in $B^0 \rightarrow K_S^0 K_S^0 K_S^0$ are compatible within two standard deviations with those measured in tree-dominated modes such as $B^0 \rightarrow J/\psi K_S^0$, as expected in the SM. CP conservation is excluded for the first time in these decay with a significance of more than 3σ , including systematic uncertainties.
- The CP asymmetry in $B^+ \rightarrow \phi K^+$ differs from 0 by 2.8σ , and is in slight tension with SM predictions ($0-4.7\%$).
- The amount of CP violation in $B^0 \rightarrow \phi K_S^0$ and in other $B^0 \rightarrow K^+ K^- K_S^0$ decays is in excellent agreement with SM expectations: β_{eff} is very close to β measured in B decays to charmonium, and \mathcal{C} is consistent with zero.
- No evidence of CP violation has been found in $B^\pm \rightarrow K^*(892)^\pm \pi^0$, though the large uncertainty on the CP asymmetry does not exclude CP -violating effects as large as $20-30\%$, as expected in the SM.
- No evidence of lepton-flavor violating $B^\pm \rightarrow h^\pm \tau \ell$ decays has been found, and upper limits of a few times 10^{-5} on their branching fractions have been set, improving by a factor 5 previous limits on $\mu - \tau$ lepton-flavor violating effective couplings.
- No evidence of $B \rightarrow \text{invisible}(+\gamma)$ decays has been found, and upper limits of a few times 10^{-5} on their branching fractions have been set, 1-2 order of magnitude still higher than the values predicted by some theoretical models beyond the SM.

All the results are in agreement with Standard Model expectations: no evidence of new physics is found.

-
- [1] N. Cabibbo, "Unitary Symmetry and Leptonic Decays", Phys. Rev. Lett. **10**, 531 (1963).
 - [2] M. Kobayashi, T. Maskawa, " CP violation in the renormalizable theory of weak interaction", Prog. Theor. Phys. **49**, 652 (1973).
 - [3] Heavy Flavor Averaging Group, <http://www.slac.stanford.edu/xorg/hfag/>
 - [4] H. J. Lipkin, "Interference effects in $K\eta$ and $K\eta'$ decay modes of heavy mesons. Clues to understanding weak transitions and CP violation", Phys. Lett. B **254**, 247 (1991).
 - [5] M. Bander, D. Silverman, and A. Soni, " CP Noninvariance in the Decays of Heavy Charged Quark Systems", Phys. Rev. Lett. **43**, 242 (1979).
 - [6] H.-Y. Cheng and C.-K. Chua, "Revisiting charmless hadronic $B_{u,d}$ decays in QCD factorization", Phys. Rev. D **80**, 114008 (2009).
 - [7] Z. J. Xiao, Z. Q. Zhang, X. Liu, and L. B. Guo, "Branching ratios and CP asymmetries of $B \rightarrow K\eta^{(\prime)}$ decays in the pQCD approach," Phys. Rev. D **78**, 114001 (2008).
 - [8] H. S. Wang, X. Liu, Z. J. Xiao, L. B. Guo, and C. D. Lu, "Branching ratio and CP asymmetry of $B \rightarrow \pi\eta^{(\prime)}$ decays in the perturbative QCD approach," Nucl. Phys. B **738**, 243 (2006).
 - [9] A.G. Akeroyd, C.H. Chen, and C.Q. Geng, " $B \rightarrow \eta^{(\prime)}(l^-\bar{\nu}, l^+l^-, K, K^*)$ decays in the quark-flavor mixing scheme", Phys. Rev. D **75**, 054003 (2007).
 - [10] A. R. Williamson and J. Zupan, "Two body B decays with isosinglet final states in SCET," Phys. Rev. D **74**, 014003 (2006) [Erratum-ibid. D **74**, 039901 (2006)].
 - [11] M. Beneke and M. Neubert, "Flavor-singlet B decay amplitudes in QCD factorization," Nucl. Phys. B **651**, 225 (2003).
 - [12] C.-W. Chiang, M. Gronau, J. L. Rosner and D. A. Suprun, "Charmless $B \rightarrow PP$ decays using flavor SU(3) symmetry," Phys. Rev. D **70**, 034020 (2004).
 - [13] Belle Collaboration, C.-T. Hoi *et al.*, "Evidence for direct CP violation in $B^\pm \rightarrow \eta h^\pm$ and observation of $B^0 \rightarrow \eta K^0$ ", Phys. Rev. Lett. **108**, 031801 (2012).

- [14] H.-Y. Cheng, C.-K. Chua, and A. Soni “ CP -violating asymmetries in B^0 decays to $K^+K^-K_{S(L)}^0$ and $K_S^0K_S^0K_{S(L)}^0$ ”, Phys. Rev. D **72**, 094003 (2005).
- [15] M. Beneke, “Corrections to $\sin 2\beta$ from CP asymmetries in $B^0 \rightarrow (\pi^0, \rho^0, \eta, \eta', \omega, \phi)K_S^0$ decays”, Phys. Lett. B **620**, 143 (2005).
- [16] H.-n. Li and S. Mishima, “Penguin-dominated $B \rightarrow PV$ decays in NLO perturbative QCD”, Phys. Rev. D **74**, 094020 (2006).
- [17] BABAR Collaboration, J. P. Lees *et al.*, “Amplitude analysis and measurement of the time-dependent CP asymmetry of $B^0 \rightarrow K_S^0K_S^0K_S^0$ decays,” Phys. Rev. D **85**, 054023 (2012).
- [18] BABAR Collaboration, B. Aubert *et al.*, “Dalitz plot analysis of the decay $B^\pm \rightarrow K^\pm K^\pm K^\mp$,” Phys. Rev. D **74**, 032003 (2006).
- [19] BABAR Collaboration, J. P. Lees *et al.*, “Study of CP violation in Dalitz-plot analyses of $B^0 \rightarrow K^+K^-K_S^0$, $B^+ \rightarrow K^+K^-K^+$, and $B^+ \rightarrow K_S^0K_S^0K^+$,” Phys. Rev. D **85**, 112010 (2012).
- [20] Q. Chang, X.-Q. Li, and Y.-D. Yang, “Revisiting $B \rightarrow \pi K$, πK^* and ρK decays: CP violations and implication for new physics”, J. High Energy Phys. **09** (2008) 038.
- [21] C.-W. Chiang and D. London, “Looking for new physics in $B \rightarrow K^*\pi$ and $B \rightarrow \rho K$ decays”, Mod. Phys. Lett. A **24**, 1983 (2009).
- [22] M. Gronau, D. Pirjol, and J. Zupan, “ CP asymmetries in $B \rightarrow K\pi, K^*\pi, \rho K$ decays”, Phys. Rev. D **81**, 094011 (2010).
- [23] BABAR Collaboration, J. P. Lees *et al.*, “Observation of the rare decay $B^+ \rightarrow K^+\pi^0\pi^0$ and measurement of the quasi-two-body contributions $B^+ \rightarrow K^*(892)^+\pi^0$, $B^+ \rightarrow f_0(980)K^+$, and $B^+ \rightarrow \chi_{c0}K^+$ ”, Phys. Rev. D **84**, 092007 (2011).
- [24] X.-G. He, G. Valencia, and Y. Wang, “Lepton flavor violating τ and B decays and heavy neutrinos”, Phys. Rev. D **70**, 113011 (2004).
- [25] M. Sher and Y. Yuan, “Rare B decays, rare τ decays, and grand unification”, Phys. Rev. D **44**, 1461 (1991).
- [26] D. Black, T. Han, H.-J. He, and M. Sher, “ $\tau - \mu$ flavor violation as a probe of the scale of new physics”, Phys. Rev. D **66**, 053002 (2002).
- [27] T. Fujihara, S.K. Kang, C. S. Kim, D. Kimura, and T. Morozumi, “Low scale seesaw model and lepton flavor violating rare B decays”, Phys. Rev. D **73**, 074011 (2006).
- [28] BABAR Collaboration, J. P. Lees *et al.*, “Search for the decay modes $B^\pm \rightarrow h^\pm\tau\ell$,” Phys. Rev. D **86**, 012004 (2012).
- [29] G. Buchalla and A. J. Buras, “QCD corrections to rare K and B decays for arbitrary top quark mass”, Nucl. Phys. B **400**, 225 (1993).
- [30] C. D. Lu and D. X. Zhang, “ $B_s(B_d) \rightarrow \gamma\gamma\bar{\nu}$ ”, Phys. Lett. B **381**, 348 (1996).
- [31] A. Dedes, H. Dreiner, and P. Richardson, “Attempts at explaining the NuTeV observation of dimuon events”, Phys. Rev. D **65**, 015001 (2002).
- [32] K. Agashe and G.-H. Wu, “Remarks on models with singlet neutrino in large extra dimensions”, Phys. Lett. B **498**, 230 (2001).
- [33] H. Davoudiasl, P. Langacker, and M. Perelstein, “Constraints on large extra dimensions from neutrino oscillation experiments”, Phys. Rev. D **65**, 105015 (2002).
- [34] Belle Collaboration, C. L. Hsu *et al.*, “Search for B^0 decays to invisible final states,” Phys. Rev. D **86**, 032002 (2012).
- [35] BABAR Collaboration, J. P. Lees *et al.*, “Improved Limits on B^0 Decays to Invisible Final States and to $\nu\bar{\nu}\gamma$,” arXiv:1206.2543 [hep-ex]. Submitted to Phys. Rev. D.
- [36] charge conjugate modes are implicitly included unless otherwise stated